INTERNATIONAL JOURNAL FOR NUMERICAL METHODS IN FLUIDS
*Int. J. Numer. Meth. Fluids* 2002; **39**:533–548 (DOI: 10.1002/fld.343)

# Design optimization of axial flow hydraulic turbine runner: Part II—multi-objective constrained optimization method

Guoyi Peng[1,*,†], Shuliang Cao[2], Masaru Ishizuka[1] and Shinji Hayama[1]

[1] *Department of Mechanical Systems Engineering, Faculty of Engineering, Toyama Prefectural University, 5180 Kurokawa, Kosugi-machi, Imizu-gun, Toyama 939-0398, Japan*
[2] *Department of Thermal Engineering, Tsinghua University, Beijing 100084, China*

SUMMARY

This paper is concerned with the design optimization of axial flow hydraulic turbine runner blade geometry. In order to obtain a better design plan with good performance, a new comprehensive performance optimization procedure has been presented by combining a multi-variable multi-objective constrained optimization model with a Q3D inverse computation and a performance prediction procedure. With careful analysis of the inverse design of axial hydraulic turbine runner, the total hydraulic loss and the cavitation coefficient are taken as optimization objectives and a comprehensive objective function is defined using the weight factors. Parameters of a newly proposed blade bound circulation distribution function and parameters describing positions of blade leading and training edges in the meridional flow passage are taken as optimization variables.

The optimization procedure has been applied to the design optimization of a Kaplan runner with specific speed of 440 mkW. Numerical results show that the performance of designed runner is successfully improved through optimization computation. The optimization model is found to be validated and it has the feature of good convergence. With the multi-objective optimization model, it is possible to control the performance of designed runner by adjusting the value of weight factors defining the comprehensive objective function. Copyright © 2002 John Wiley & Sons, Ltd.

KEY WORDS: fluid machinery; hydraulic turbine; Kaplan runner blades; inverse problem; design optimization; computational fluid dynamics

## 1. INTRODUCTION

The inverse computation of hydraulic turbine runner is to design a blade geometry corresponding to specified design parameters. It is a complex problem of non-linear programming. Traditional design is usually performed under certain design specifications given empirically. For the difficulty of defining those design specifications, which have a great influence on runner performance, a design obtained by conventional methods is only one of feasible plans

* Correspondence to: Guoyi Peng, Department of Mechanical Systems Engineering, Faculty of Engineering, Toyama Prefectural University, 5180 Kurokawa, Kosugi-machi, Imizu-gun, Toyama 939-0398, Japan.
† E-mail: peng@pu-toyama.ac.jp

*Received April 2001*
*Revised December 2001*

rather than the best one. Thus, a better design of good performance is usually selected through performance experiments of many designed runners. It will take much time and cost to design a runner of good performance with conventional methods.

As the development of computational fluid dynamics, some powerful new inverse design models have been proposed and much progress has been made with the performance prediction of hydraulic runner blades by numerical methods. It becomes possible to search a better design plan numerically by combining an inverse computation and a performance prediction procedure with optimization algorithms. Concerning the design optimization of blade geometry, many efforts have been made and the method of first optimizing blade loading distribution and then using an inverse shape design to obtain the actual optimized blade shape is well developed and practiced for a long time [1, 2]. Massado and Satta studied the design optimization of axial flow compressor using simple pitchline analysis [3]. Their work shows that the comprehensive performance design optimization of turbomachinery runner is much complicated for the difficulty to describe mathematically the effect of blade geometry design specifications on the performance of runner blades. Considering the practice of hydraulic runner blade, the present work tries to construct a comprehensive performance optimization procedure for the geometry design of Kaplan turbine runner blades based on a three-dimensional inverse computation of quick convergence.

The objective of inverse computation is to design a runner having good performance. In general, a hydraulic turbine runner of good performance should: (1) satisfy the requirements of given design parameters, (2) have a high efficiency under the optimum working condition and a relative wide high-efficiency range of working, (3) have a good cavitation performance, and (4) have a good hydro-dynamic stability. Except the main quality indexes given above, there are some other quality indexes related to special working conditions. It is to say that the performance of hydraulic runner should be evaluated from the many quality indexes. But it is difficult to express all the quality indexes mathematically. So, only the main quality indexes of the efficiency performance and the cavitation performance of Kaplan runner are considered in this paper because the main purpose of the present work is to demonstrate a feasibility of comprehensive design optimization for engineering practice.

For a comprehensive performance design optimization of hydraulic turbine runner, besides the optimization algorithm of quick convergence, following items are also essential. The first is an effective inverse computation model to design blade geometry. The second is a reliable direct numerical simulation procedure of flow analysis. The third is a truthful mathematical model evaluating runner performance based on direct flow analysis. As for the inverse design of turbomachinery blades, there are some useful fully three-dimensional (F3D) [4–6] and quasi-three-dimensional (Q3D) [7–9] inverse computation models, and they have been gradually used for the engineering practice. Compared with the F3D inverse model [10, 11], the improved Q3D inverse model reported in part I [12] has the feature of quick convergence. As shown in Figure 1, the flow computation is made from the far inlet of guide vanes to the far outlet of runner by solving a set of governing equations simultaneously in the Q3D method. So influences of guide vane parameters and the geometry of meridional flow passage on the design of runner have been taken into account. The difficulty of defining the flow condition at the blade inlet, which is essential to conventional methods, is surmounted. Although an assumption of symmetric flow has been made, the inverse method has a sufficient accuracy for the engineering practice. Concerning the computer time of iterative computations, the improved Q3D inverse model is adopted in the present design optimization procedure.

 

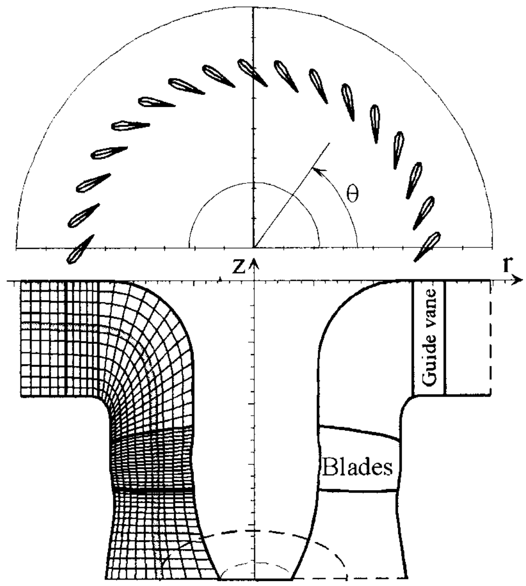


Figure 1. Schematic representation of Kaplan turbine and computation domain.

As for the flow analysis, many computation results have been reported [13, 14]. Although it is possible to simulate the flow in hydraulic turbines by solving RANS equations directly, it is much time consuming. Experimental research shows that the effect of fluid viscosity is limited within a thin layer close to the solid boundaries [15]. Therefore, the flow in hydraulic turbine is usually analysed by iteration computations of inviscid main flow and boundary layers in engineering practice. For the above reasons, the performance estimation of the designed runner is based on a combination computation of inviscid main flow and viscous boundary layers [16, 17] in the present procedure. The inviscid main flow is computed by solving steady Euler equations considering that the boundary displacement defined by the calculation of boundary layers, and the three-dimensional boundary layers in the runner blades are calculated using the integral method according to the velocity and pressure distributions of outer layer given through inviscid flow analysis. Effects of fluid viscosity such as losses, flow transition and flow separation are estimated in the process of boundary layer calculations. The elevation of runner blades to be designed is thought to be low enough. So the runner cavitation coefficient representing the performance of runner blades is always smaller than the Thomas cavitation coefficient representing the critical value of cavitation inception. Thus, cavitations can be neglected in the process of direct flow analysis. By combining the above procedures with a multi-objective constrained optimization model a comprehensive performance optimization procedure shown in Figure 2 is proposed for axial flow hydraulic turbine runner design.

## 2. MULTI-OBJECTIVE DESIGN OPTIMIZATION OF KAPLAN RUNNER

An optimization procedure consists of objective functions, optimization variables as well as the needed constraints. These are dependent on special problems. Concerning the design of axial

 

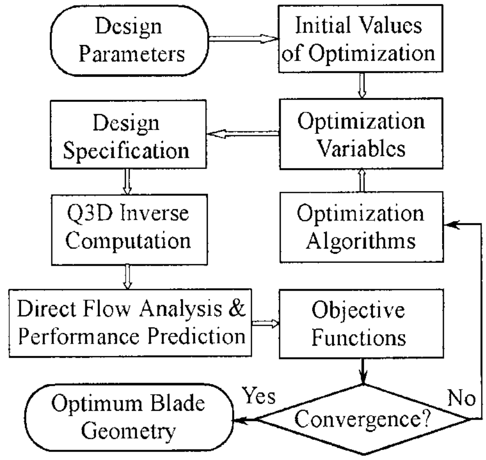


Figure 2. Routine of design optimization of hydraulic blades.

flow hydraulic turbine runner, objective functions are determined from the main quality indexes and the optimization variables are taken from parameters describing design specification. By analysing the inverse design of axial flow hydraulic turbine runner, the following mathematical model of optimization is proposed.

### 2.1. *Objective functions*

As stated in proceed section the performance of hydraulic runner is a comprehensive evaluation of many quality indexes. It is difficult to define a mathematical expression of quantity for every quality index. Although there are many quality indexes and some special request for a special project, the hydraulic efficiency performance and cavitation performance are generally the main ones. So the comprehensive performance of designed runner is evaluated from the hydraulic efficiency performance and the cavitation performance in this computation. Concerning hydraulic efficiency, an objective function, $F_\eta(X)$ is taken to be the total hydraulic loss that is estimated through the three-dimensional boundary layer computations [16, 17]

$$F_\eta(X) = 1 - \zeta(X) \tag{1}$$

where $\zeta$ denotes the hydraulic efficiency and $X$ a vector of optimization variables.

Cavitation in hydraulic turbines may occur on the suction surfaces of runner blades where the dynamic action of blades acting on the fluid creates low pressure zones in a region where the static pressure is already low. Cavitations will commence when the local static pressure is less than the vapour pressure of water, i.e. where the head is low, the velocity is high and the elevation of the turbine is set too high above the tailrace. According to the characteristics of cavitation inception, the cavitation performance of hydraulic turbines is correlated with a runner cavitation coefficient (or cavitation number), $\sigma$, defined as

$$\sigma = \lambda K_W^2 + \zeta_t K_V^2 \tag{2}$$

 

where

$$\lambda = (W_k/W_0)^2 - 1, \quad K_W = W_0/\sqrt{2gH}, \quad K_V = V_0/\sqrt{2gH}$$

in which $W_k$ denotes the relative velocity at the location of the lowest pressure, $H$ the effective head, $g$ the gravity, $W_0$ and $V_0$ the mean relative velocity and the mean absolute velocity at the exit of runner blades, respectively, $\zeta_t$ is the efficiency of the draft tube. Related to the elevation of runner blades, the Thoma coefficient, $\sigma_z$, is usually defined as

$$\sigma_z = (p_a - \rho g H_s - p_v)/(\rho g H) \tag{3}$$

where $H_s$ denotes the elevation of the runner blades above the tailrace, $\rho$ the fluid density, $p_a$ and $p_v$ the atmospheric pressure and the vapor pressure of water, respectively [18]. When the runner cavitation coefficient is greater than the Thoma coefficient that represents the fraction of head available for the production of work, cavitation inception will occur in runner blades. So, a hydraulic runner of good cavitation performance should have a cavitation coefficient as small as possible under a certain efficiency. Thus, the optimization objective function of cavitation performance, $F_\sigma(X)$, is directly taken to be the runner cavitation coefficient in the present computation:

$$F_\sigma(X) = \sigma(X) \tag{4}$$

### 2.2. Optimization variables

Optimization variables should be determined from design parameters, which can be classified as basic design parameters and design specifications. The basic parameters of hydraulic turbine runner design are the working head $H$, the flow rate $Q$ and the rotational speed $n_d$ as well as the runner diameter $D_1$. These are the given parameters for a specific project. Thus, optimization variables should be variables describing design specification of inverse computation. For the axial flow hydraulic turbine runner, the main design specifications include the geometry of the meridional flow passage, positions of the blade leading edge and the trailing edge in the flow passage, the position of blade adjusting stem axis, the blade number, the blade thickness distribution and the blade bound circulation distribution.

The geometry of the meridional flow passage is very complex, and it will take many parameters to describe its shape mathematically. On the other hand, the geometry of meridional flow passage has got standardized gradually through engineering practice. There is only a very little change for an individual design. Concerning the capacity of computer, a standardized flow passage is adopted in this computation. The number of runner blade is an important parameter having great influence on the runner performance. But it can only take a few value of integer. It is much more cheaper to take it as a given design parameter and then to compare the performance of designed runner rather than to take it as an optimization variable. The thickness of runner blade is mainly determined by requirements of strength and manufacturing technology. Thus, the blade thickness distribution is defined according to the statistical data in this computation. The position of blade adjusting stem axis is nearly a given value for a specific project also.

The above analysis shows that the left design specifications, which should be considered in the design optimization, are the blade bound circulation distribution and positions of blade leading and trailing edges. In order to take them into optimization procedure, the following simple mathematical expressions to describe those design specifications are proposed.

 

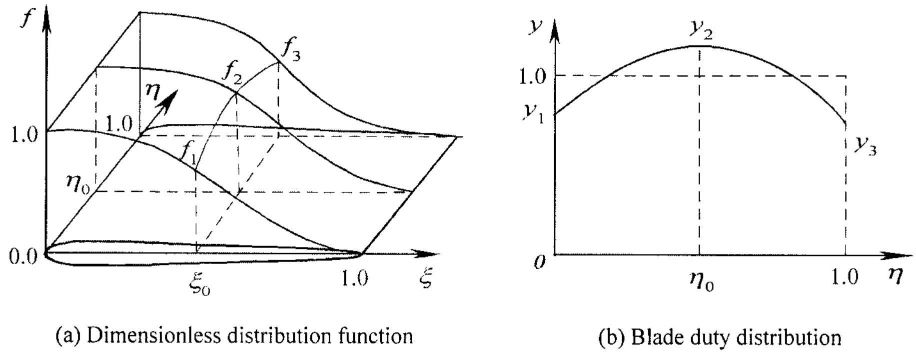


Figure 3. Velocity torque distribution in blade region.

*2.2.1. Expression of mean velocity torque distribution.* The blade bound circulation is an important design specification determining the shape of the runner blade. It is usually given by specifying a circumferentially averaged mean velocity torque distribution. For the hydraulic turbine runner, the value of velocity torque at the inlet of blade leading edge is determined by the inflow of upstream from guide vanes. The variation of velocity torque from the inlet of blade leading edge to the outlet of blade trailing edge is determined by specific blade duty of the designing runner. So the mean velocity torque distribution, $\bar{V}_\theta r$, can be expressed as follows:

$$(\bar{V}_\theta r)(z,r) = (\bar{V}_\theta r)_{0,i} - f(\xi,\eta)\Delta(\bar{V}_\theta r)_i \tag{5}$$

where $\xi(z,r)$ denotes the relative streamline co-ordinate from the blade leading edge ($\xi = 0$) to the trailing edge ($\xi = 1.0$), $\eta(z,r)$ the relative quasi-orthogonal co-ordinate from the hub ($\eta = 0$) to the tip ($\eta = 1.0$). The subscript $i$ denotes a streamline and 0 the blade inlet. $f(\xi,\eta)$ is a dimensionless distribution function and $0 \leqslant f(\xi,\eta) \leqslant 1$. $\Delta(\bar{V}_\theta r)_i$, is the variation of velocity torque from the blade inlet to the outlet along the streamline. It is usually given to be a constant value $\Delta(\bar{V}_\theta r)$, which is determined by the energy conservation

$$\Delta(\bar{V}_\theta r) = gH\zeta_{\mathrm{h}}/\omega \tag{6}$$

where $H$ denotes the work head of hydraulic runner, $\omega$ the angular velocity, $g$ the gravity and $\zeta_{\mathrm{h}}$ the hydraulic efficiency.

Concerning the distribution function $f(\xi,\eta)$, the first, its derivative in the direction of streamline should be set to zero (or a small value) at the blade trailing edge in order to satisfy the *Kutta–Joukowsky* condition. The second, its derivative in the streamline direction at blade leading edge determines the attack angle of blade inlet and is usually set to zero for a design of no-incidence. Thus, the distribution function as shown in Figure 3(a) is proposed to be a fourth-order polynomial in the streamline direction:

$$f(\xi,\eta) = \sum_{n=0}^{4} a_n(\eta)\xi^n \tag{7}$$

 

To determine parameters $(a_0, a_1, \ldots, a_4,)$ of the above expression, the following constraint conditions are introduced:

$$\frac{\mathrm{d}f}{\mathrm{d}\xi} = 0 \quad \text{and} \quad f(\xi = 0, \eta) = 0 \ \text{at} \ \xi(z, r) = 0 \quad \text{(blade leading edge)}$$
$$f(\xi = \xi_0, \eta) = f_0(\eta) \tag{8}$$
$$\frac{\mathrm{d}f}{\mathrm{d}\xi} = 0 \quad \text{and} \quad f(\xi = 1, \eta) = 0 \ \text{at} \ \xi(z, r) = 1 \quad \text{(blade trailing edge)}$$

where $\xi_0$ is the relative streamline co-ordinate of a given position and $0 < \xi_0 < 1$. $f_0(\eta)$ is a quadratic function of defining the distribution along the blade height. The quadratic function is given as

$$f_0(\eta) = \sum_{n=0}^{2} b_n \eta^n \tag{9}$$

It is subject to the following constraints:

$$f_0(0) = f_1, \quad f_0(\eta_0) = f_2, \quad f_0(1) = f_3 \tag{10}$$

where $f_1$, $f_2$ and $f_3$ are the essential dimensionless parameters to specify the distribution function. $\eta_0$ is the relative quasi-orthogonal line co-ordinate of a given position and $0 < \eta_0 < 1$. According to the above, the distribution function can be written as $f(\xi, \eta) = f(f_1, f_2, f_3)$.

As a special problem of Kaplan runner, the leakage flow of tip and hub clearances has a great influence on the runner performance. According to relative materials, the lower the pressure difference acting on the clearance, the smaller the hydraulic loss deduced by the leakage flow. Thus, a small value of blade duty near the blade tip and hub clearances is thought to be beneficial to reduce the hydraulic loss of clearance leakage flow. On the other hand, the inflow of Kaplan runner has a great gradient of $\bar{V}_\theta r$ in the span-wise direction near the tip at the blade inlet [19]. So the gradient of $\bar{V}_\theta r$ along the blade trailing edge is large for a design of constant blade duty along the blade height. This may give rise to a tailing vortex loss at runner exit [20]. A non-uniform distribution of $\Delta(\bar{V}_\theta r)_i$, along the blade height is expected to be beneficial to reduce the trailing vortex loss to some extent. On these considerations, the design of non-uniform blade duty is tried. The blade duty is defined using a distribution function as follows:

$$\Delta(\bar{V}_\theta r)_i = \kappa y(\eta) \Delta(\bar{V}_\theta r) \tag{11}$$

where $\Delta(\bar{V}_\theta r)_i$ denotes the variation of velocity torque from the blade inlet to the outlet along an arbitrary streamline denoted as $i$. $\kappa$ is a coefficient given as $\kappa = 1/\int_0^1 y(\eta)\,\mathrm{d}\eta$ to satisfy the conservation of energy. $\Delta(\bar{V}_\theta r)$ denotes the average value of blade duty given by Equation (6). $y(\eta)$ is a dimensionless distribution function. As shown in Figure 3(b), the function is supposed to be parabolic along the blade height.

$$y(\eta) = \sum_{n=0}^{2} c_n \eta^n \tag{12}$$

 

Its parameters are defined by the following constraints:

$$y(0) = y_1, \quad y(\eta_0) = y_2, \quad y(1) = y_3 \tag{13}$$

where $y_1$, $y_2$ and $y_3$ are the essential dimensionless parameters to specify the distribution. Thus, the function of the defining blade duty can be written to be $y(\eta) = y(y_1, y_2, y_3)$. Therefore, Equation (5) of defining blade bound circulation can be expressed as $(\bar{V}_\theta r)(z,r) = F(f_1, f_2, f_3, y_1, y_2, y_3)$.

*2.2.2. Description of blade leading and trailing edges.* The solidity of runner blade cascade has a great influence on the runner performance also. It is mainly determined by the position of blade leading and trailing edges under a given specified blade bound circulation distribution. Concerning the adjustment of runner blade cascade opening, the blade leading edge and the trailing edge in the flow passage should be defined to let the total hydraulic lift act around the blade stem axis.

The position of blade leading and trailing edges in meridional flow passage is usually defined empirically according to statistical data. Their geometry is complex and it will take many parameters to describe precisely. On the other hand, a simple quadratic function may give a geometry close to empirical ones to a certain extent. As the main purpose of the present work is to show a possibility of multi-variable optimization, the blade leading edge and the trailing edge in the meridional flow passage are approximately defined as quadratic curves in this computation. The function expressing the blade leading edge is written as

$$Z_{\text{in}}(\eta) = \sum_{n=0}^{2} d_n \eta^n \tag{14}$$

where the co-ordinate $z$ is set to be in the direction of runner axis and its origin is at the centre of blade stem axis. It is supposed to pass through three reference points $(0, z_1^i), (\eta_0, z_2^i)$ and $(1, z_3^i)$. Then the function can be expressed as

$$Z_{\text{in}}(\eta) = Z_{\text{in}}(z_1^i, z_2^i, z_3^i) \tag{15}$$

In the same way, the blade trailing edge can be expressed as follows by giving three reference points $(0, z_1^o)$, $(\eta_0, z_2^o)$ and $(1, z_3^o)$.

$$Z_{\text{out}}(\eta) = Z_{\text{out}}(z_1^o, z_2^o, z_3^o) \tag{16}$$

To decrease the number of parameters, the following approximate relations from statistical data is further introduced [21].

$$z_1^o = -\frac{0.55}{0.45} z_1^i, \quad z_2^o = -\frac{0.55 + 0.05\eta_0}{0.45 - 0.05\eta_0} z_2^i, \quad z_3^o = -\frac{0.6}{0.4} z_3^i \tag{17}$$

By this way, we reach $\{Z_{\text{in}}, Z_{\text{out}}\} = F(z_1^i, z_2^i, z_3^i)$. The number of parameters describing blade leading and trailing edges is reduced to three.

### *2.3. Constraints of Kaplan runner design*

The basic constraint of hydraulic runner design is the conservation of energy. This principle has been always satisfied in the inverse computation by defining a proper mean velocity torque distribution by Equation (5) with the given method. Besides, the inverse computation should also suffer from some constraints for flow property and runner geometry corresponding to special requirements. According to the characteristics of Kaplan turbine, the following constraints are adopted:

The first is a constraint of flow separation. It is written as

$$G_1(X) = -(T + 0.06) \leqslant 0 \tag{18}$$

where $T$ is the approximate criterion for flow separation given as follows:

$$T = \frac{\delta R_{e\delta}^{1/4}}{W} \frac{\mathrm{d}W}{\mathrm{d}s}$$

in which $R_{e\delta} = \delta W/v$, $\delta$ denotes the momentum thickness of boundary layer, $v$ the fluid kinematic viscosity, $W$ the relative velocity of the main flow at the edge of the boundary, and $s$ the stream line [21, 22].

The second, in order to guarantee the designed blade to work at turbine status everywhere, the following flow constraint is also introduced:

$$G_2(X) = W_\mathrm{p} - W_\mathrm{s} \leqslant 0 \tag{19}$$

where subscripts p and s denote the pressure surface and the suction surface of the blade, respectively.

The third, the blade row solidity is an important geometry parameter to the runner blades arranged in cascade. The increase of blade row solidity allows an increase in blade loading, but the viscous friction loss also increases. For the particularity of Kaplan runner blades, the solidity of blade cascade is usually specified to decrease monotonically from the hub to the tip [18]. Thus, the following constraint concerning the blade row solidity is also adopted in the present optimization

$$G_3(X) = \frac{\mathrm{d}(L/t)}{\mathrm{d}\eta} \leqslant 0 \tag{20}$$

where $L/t$ denotes the solidity of runner blades cascade, in which $L$ and $t$ are the length of blade chord and the length of pitch of the blade row, respectively.

### 2.4. Mathematical model of design optimization

Through the above analysis, we know that the comprehensive performance optimization of Kaplan runner is a multi-variable multi-objective constrained problem written as follows:

$$\begin{aligned} &\min[F_\eta(X), F_\sigma(X)]^\mathrm{T} \\ &\{G_i(X) \leqslant 0,\ i = 1, 2, \ldots, m\} \end{aligned} \tag{21}$$

where $G_i(X)$ denotes all constraints of inequality and equality. Optimization variables should be the parameters defining design specifications. They are denoted as follows:

$$X = \{f_1, f_2, f_3, z_1^i, z_2^i, z_3^i, y_1, y_2, y_3\}^\mathrm{T} \tag{22}$$

 

These variables are constrained within a reasonable range by introducing the flowing constraint conditions:

$$\begin{aligned} G_4(X) &= \{x_i^{\mathrm{l}} - x_i \leqslant 0,\ \ i = 1, 2, \ldots, n\} \\ G_5(X) &= \{x_i - x_i^{\mathrm{u}} \leqslant 0,\ \ i = 1, 2, \ldots, n\} \end{aligned} \tag{23}$$

where $x_i^{\mathrm{l}}$ and $x_i^{\mathrm{u}}$ are the lower and upper limitations.

For numerical evaluation of the optimization objective, a comprehensive objective function, $F(X)$, is defined as follows using the weight factors:

$$F(X) = \omega_{1\eta}\omega_{2\eta}F_\eta(X) + \omega_{1\sigma}\omega_{2\sigma}F_\sigma(X) \tag{24}$$

where $\omega_{1\eta}$ and $\omega_{1\sigma}$ denote weight factors concerning the importance of sub-objectives and $\omega_{1\eta} + \omega_{1\sigma} = 1.0$. $\omega_{2\eta}$ and $\omega_{2\sigma}$ denote weight factors concerning the order of sub-objective measuring units. In general,

$$\omega_{2\eta} = \frac{1}{\min F_\eta(X)}, \quad \omega_{2\sigma} = \frac{1}{\min F_\sigma(X)} \tag{25}$$

In this way, the above multi-objective optimization is simplified to a multi-variable constrained optimization of single objective.

$$\begin{aligned} &\min F(X) \\ &g_i(X) < 0 \quad (i = 1, 2, \ldots, m) \\ &h_j(X) = 0 \quad (j = 1, 2, \ldots, l) \end{aligned} \tag{26}$$

where $g_i(X)$ and $h_j(X)$ denote constraints of inequality and equality, respectively. The comprehensive objective function and constrain functions are covert functions of optimization variables and they are not differentiable. Therefore, the direct SWIFT (sequential weight increasing factor technique) method is adopted in the numerical procedure [23, 24]. The constrained optimization is transferred to a simple non-constrained problem using the penalty method. The augmented objective function is given as follows:

$$\min P(X, r_k) = F(X) + r_k \left\{ \sum_i^m (\max(0, g_i(X))^2 + \sum_j^l h_j^2(X) \right\} \tag{27}$$

where the penalty factor $r_k$ is defined as

$$r_k = \max\{r_k, 1/d\} \tag{28}$$

in which

$$d = \frac{1}{N+1} \sum_{i=1}^{N+1} \|X_i - X_G\| \quad \text{and} \quad X_G = \frac{1}{N+1} \sum_{i=1}^{N+1} X_i$$

where $X_i$ denotes a vector composed of optimization variables and $X_0$ the initial one. $N$ denotes the numbers of vectors composed of optimization variables with different values. This non-constrained optimization problem is then solved by Powell's conjugate direction method [25].

 

Concerning the convergence of computations, a relative error of augmented object function is defined as follows:

$$\delta_0 = |(P^{(n+1)}(X, r_k) - P^{(n)}(X, r_k))/P^{(n+1)}(X, r_k)| \tag{29}$$

where the superscript $n+1$ and $n$ denote the values of the new step and the previous step, respectively.

## 3. NUMERICAL RESULTS AND DISCUSSIONS

The present model is applied to the design optimization of a Kaplan runner named ZZ440. Design parameters of the turbine runner are given as: $n_s = 440$ mkW, $Q_d = 1.150$ m$^3$/s, $n_d = 120$r/min, $H = 1.0$m, $D_1 = 1.0$m, $B_N = 6$. The meridional passage is given as that shown in Figure 1.

First, numerical properties of the optimization model are investigated through a simple design optimization, where optimization variables are taken as $X = \{f_1, f_2, f_3\}^{\mathrm{T}}$, the objective function is taken as $\min F_\eta(X)$. It is an optimization of hydraulic efficiency performance only concerning the mean velocity torque distribution along streamline. The blade duty $\Delta\bar{V}_\theta r$ is set to be uniform along the blade height, and the blade leading and trailing edges are given as shown in Figure 1. The convergence criterion is taken as the relative error of objective function, $\delta_0 \leqslant \varepsilon$, where the accuracy of convergence accuracy, $\varepsilon = 0.5 \times 10^{-3}$. The iteration relaxation factor $\lambda = 0.25$. Under the above conditions, the numbers of iterations is about 15–20 corresponding to the initial values. Table I shows computational results under different initial values of optimization variables. These results show that the initial values of optimization variables have very little influence on the optimization result. Figure 4 shows the convergence history of optimization. The optimization procedure is found to have a good convergence and the computational result is reliable.

Second, the effect of optimization variables is investigated through computations, where the optimization objective is taken to be $\min F_\eta(X)$ and the optimization variables are, respectively, taken to be $X = \{f_1, f_2, f_3\}^{\mathrm{T}}$, $X = \{f_1, f_2, f_3, z_1^i, z_2^i, z_3^i\}^{\mathrm{T}}$, $X = \{f_1, f_2, f_3, z_1^i, z_2^i, z_3^i, y_1, y_2, y_3\}^{\mathrm{T}}$. Under a given convergence accuracy of $\varepsilon = 1.0 \times 10^{-3}$, optimization computations reach convergence after 10–50 iterations corresponding to the numbers of optimization variables. Table II shows results of hydraulic efficiency optimization for different optimization variables. It shows that the efficiency performance of the designed runner has been successfully improved by

Table I. Effect of initial value on optimization ($\varepsilon = 0.05\%$).

| | Initial | Final | Initial | Final | Initial | Final |
|---|---|---|---|---|---|---|
| $f_1$ | 0.60 | 0.47 | 0.50 | 0.47 | 0.40 | 0.48 |
| $f_2$ | 0.50 | 0.64 | 0.50 | 0.67 | 0.50 | 0.67 |
| $f_3$ | 0.40 | 0.72 | 0.50 | 0.70 | 0.60 | 0.70 |
| $F_\eta$ | $6.27 \times 10^{-2}$ | $5.22 \times 10^{-2}$ | $5.85 \times 10^{-2}$ | $5.21 \times 10^{-2}$ | $5.63 \times 10^{-2}$ | $5.22 \times 10^{-2}$ |
| $F_\sigma$ | 0.495 | 0.477 | 0.487 | 0.481 | 0.474 | 0.480 |
| $F(X)$ | 0.6272 | 0.5122 | 0.5852 | 0.5214 | 0.5629 | 0.5223 |

 

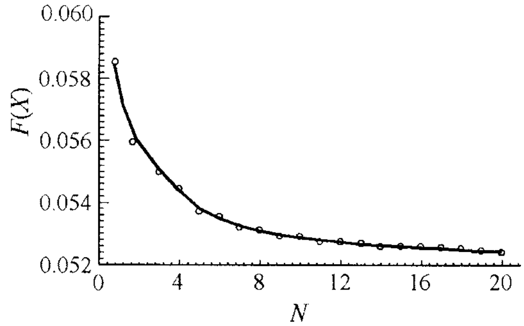


Figure 4. Convergence history of optimization procedure.

Table II. Effect of optimization variables on optimization ($\varepsilon = 0.1\%$).

| | Initial | Final | Initial | Final | Initial | Final |
|---|---|---|---|---|---|---|
| $f_1$ | 0.40 | 0.43 | 0.40 | 0.42 | 0.40 | 0.42 |
| $f_2$ | 0.50 | 0.53 | 0.50 | 0.54 | 0.50 | 0.52 |
| $f_3$ | 0.60 | 0.72 | 0.60 | 0.59 | 0.60 | 0.61 |
| $z_1^i$ | 0.397 | | 0.397 | 0.380 | 0.397 | 0.323 |
| $z_2^i$ | 0.287 | | 0.287 | 0.253 | 0.287 | 0.226 |
| $z_3^i$ | 0.208 | | 0.208 | 0.222 | 0.208 | 0.224 |
| $y_1$ | 1.00 | | 1.00 | | 1.00 | 0.95 |
| $y_2$ | 1.00 | | 1.00 | | 1.00 | 1.20 |
| $y_3$ | 1.00 | | 1.00 | | 1.00 | 0.80 |
| $F_\eta$ | $5.63 \times 10^{-2}$ | $5.23 \times 10^{-2}$ | $5.63 \times 10^{-2}$ | $4.76 \times 10^{-2}$ | $5.63 \times 10^{-2}$ | $4.33 \times 10^{-2}$ |
| $F_\sigma$ | 0.474 | 0.484 | 0.474 | 0.822 | 0.474 | 0.627 |
| $F(X)$ | 0.5629 | 0.5531 | 0.5629 | 0.4761 | 0.5629 | 0.4325 |

optimizing the velocity torque distribution. By optimizing those variables defining the shape of blade leading and trailing edges, the performance of the designed runner is improved much more. Compared to the design of constant blade duty along the blade height ($y_1 = y_2 = y_3 = 1.0$), the design optimization of non-constant blade duty improves the runner performance to some extent. For the flow complexity, it is difficult to evaluate the effect of a non-constant blade duty on runner performance. The new design of non-constant duty along the blade height needs to be researched further on the base of hub and tip clearance leakage flow investigation.

Figure 5 shows the optimized dimensionless distribution function defining the average velocity torque distribution. Corresponding to the distribution function, the $\bar{V}_\theta r$ distribution along streamlines from the blade inlet to the outlet obtained through optimization computation is shown in Figure 6. Figure 7 shows the shape of blade leading and trailing edges in the meridional flow passage, where dash lines show initial geometry of blade leading and trailing edges and solid lines the optimized ones. Figure 7 shows also the contours of $\bar{V}_\theta r$ distribution in the blade region after optimization computations by fine solid lines. It demonstrates a strong gradient in the span direction near the tip, which affects the convergence

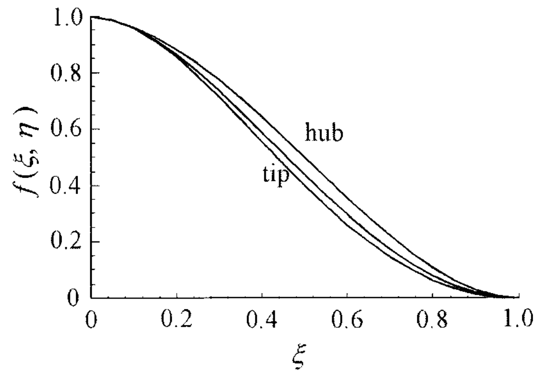


Figure 5. Optimized dimensionless distribution function.

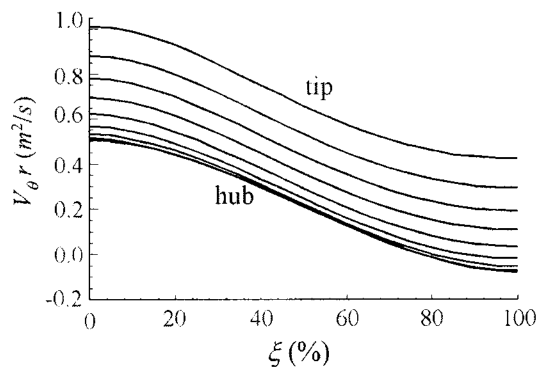


Figure 6. Optimized velocity torque distribution along streamlines.

of design optimization greatly. Figure 8 shows the geometry of runner blade on cylindrical sections obtained through design optimization. The blade is found to be smoothing and reasonable.

Third, the effect of weight factors is investigated through computations of multi-objective optimization. Table III shows computational results for different values of weight factors, where the blade duty is given to be constant along the blade height ($y_1 = y_2 = 1.0$). When $\omega_{1\eta} = 1.0$ and $\omega_{1\sigma} = 0.0$, the objective functions becomes the total hydraulic loss only. So, the hydraulic efficiency performance is improved but the cavitation coefficient becomes greater. When $\omega_{1\eta} = 0.0$ and $\omega_{1\sigma} = 1.0$, objective functions become the cavitation coefficient only. So, the cavitation performance is improved but the hydraulic loss becomes greater. When $\omega_{1\eta} = 0.5$ and $\omega_{1\sigma} = 0.5$ objective functions include both of sub-objective functions. The defined comprehensive performance is improved through optimization of all sub-objectives. The above results show that it is possible to control the performance of designing runner by adjusting the value of weight factors.

 

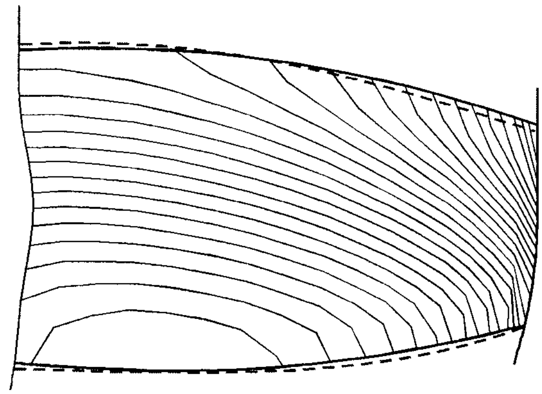


Figure 7. Shape of blade leading and trailing edges after optimization.

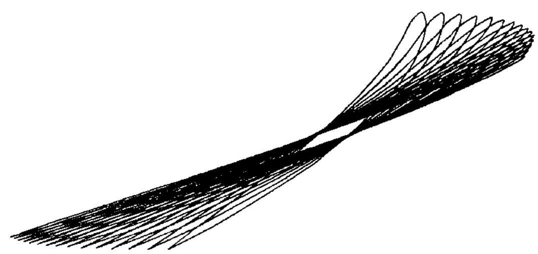

Figure 8. Geometry of designed blade on cylindrical sections.

Table III. Results of multi-objective optimization ($\varepsilon = 0.1\%$).

| | $\omega_{1\eta} = 1.0,\ \omega_{1\sigma} = 0.0$ | | $\omega_{1\eta} = 0.5,\ \omega_{1\sigma} = 0.5$ | | $\omega_{1\eta} = 0.0,\ \omega_{1\sigma} = 1.0$ | |
|---|---|---|---|---|---|---|
| | Initial | Final | Initial | Final | Initial | Final |
| $f_1$ | 0.40 | 0.42 | 0.40 | 0.41 | 0.40 | 0.51 |
| $f_2$ | 0.50 | 0.54 | 0.50 | 0.50 | 0.50 | 0.37 |
| $f_3$ | 0.60 | 0.59 | 0.60 | 0.60 | 0.60 | 0.58 |
| $z_1^i$ | 0.397 | 0.380 | 0.397 | 0.397 | 0.397 | 0.430 |
| $z_2^i$ | 0.287 | 0.253 | 0.287 | 0.288 | 0.287 | 0.370 |
| $z_3^i$ | 0.208 | 0.222 | 0.208 | 0.208 | 0.208 | 0.240 |
| $F_\eta$ | $5.62 \times 10^{-2}$ | $4.76 \times 10^{-2}$ | $5.62 \times 10^{-2}$ | $5.59 \times 10^{-2}$ | $5.62 \times 10^{-2}$ | $7.94 \times 10^{-2}$ |
| $F_\sigma$ | 0.474 | 0.822 | 0.474 | 0.459 | 0.474 | 0.402 |
| $F(X)$ | 0.5616 | 0.4761 | 0.5182 | 0.5090 | 0.4743 | 0.4021 |

 

## 4. CONCLUSIONS

A multi-variable multi-objective constrained optimization model has been proposed for the Kaplan runner design in which the total hydraulic loss and the cavitation coefficient are taken as sub-objective functions, parameters describing the blade bound circulation distribution as well as the blade leading and trailing edges in meridional flow passage are taken as optimization variables.

Combined with an improved Q3D inverse computation model and a performance prediction procedure, the optimization model has been applied to the comprehensive performance optimization of Kaplan runner. Numerical results show that the present optimization procedure has the feature of good convergence. The performance of the designed runner has been successfully improved through the optimization procedure. With the present model, it is possible to control the performance of designing runner by adjusting the value of weight factors.

A function of six variables has been proposed to describe the average mean velocity torque distribution in hydraulic turbines. Its validation has been proved by the fact that the designed runner blade is smooth and rational. With this distribution function, it is very convenient to define a mean velocity torque distribution for the inverse computation.

## REFERENCES

1. Obayashi S, Takanashi S, Matsushima K. Genetic optimization of target pressure distributions for inverse design methods. *AIAA Paper* 95-078, San Diego, 1995.
2. Van Egimond JA. Numerical optimization of target pressure distributions for subsonic and transonic airfoil design. *AGARD-CP*-463, Norway, 1989.
3. Massardo A, Satta A. Axial flow compressor design optimization: Part I—Pitchline analysis and multivariable objective function influence. *ASME Transactions Journal of Turbomachinery* 1990; **112**:115–121.
4. Borges JE. A three-dimensional inverse method for turbomachinery: Part I—Theory. *ASME Transactions Journal of Turbomachinery* 1990; **112**:346–354.
5. Dang TQ. A fully three-dimensional inverse method for turbomachinery blading in transonic flows. *ASME Transactions Journal of Turbomachinery* 1993; **115**:354–361.
6. Zangeneh M, Goto A, Takemura T. Suppression of secondary flows in a mixed flow pump impeller by application of 3D inverse design method: Part 1—Design and numerical validation. *Transactions ASME Journal of Turbomachinery* 1996; **118**:536–543.
7. Schilling R, Ritzinger S. Numerical and experiment flow analysis in centrifugal pump impellers. *Proceedings of the JSME International Conference on Fluid Engineering*, Tokyo, 1997; 207–212.
8. Peng G, Fujikawa S, Cao S, Lin R. An advanced three-dimensional inverse model for the design of hydraulic machinery runner. *Proceedings of the ASME/JSME Joint Fluid Engineering Conference*, 1998; ASME FED-vol. 245: FEDSM98-4867.
9. Peng G, Fujikwa S, Cao S. An advanced quasi-three-dimensional inverse computation model for axial flow pump impeller design. *Proc. XIX IAHR Symp- Hydraulic Machinery and Cavitation*. World Scientific: Singapore, 1998; 722–733.
10. Peng G, Lin R. A three-dimensional inverse method for the design of hydraulic runner with rotational coming flow. In *Fluid Machinery*, ASME FED-vol. 222, Roratgi US, Ogut A, Hayami H (eds), ASME: New York, 1995; 161–166.
11. Peng G, Cao S, Ishizuka M, Hayama S. Fully three-dimensional inverse computation of hydraulic impeller using finite element method. *Computational Fluid Dynamics Journal* 2001; **10**:247–254.
12. Peng G, Cao S, Ishizuka M, Hayama S. Design optimization of axial flow hydraulic turbine runner Part I: An improved Q3D inverse method. *International Journal for Numerical Methods in Fluids* 2002; **39**:517–531.
13. Wang QH, Zhu GX, Wu CH. Quasi-three dimensional and fully three-dimensional rotational flow calculation in turbomachines. *ASME Transactions Journal of Engineering for Gas Turbine and Power* 1985; **107**:227–285.
14. Dawes WN. The development of a 3D Navier–Stokes solver for application to all type of turbomachinery. *ASME paper* 88-GT-70, 1988.
15. Schachenmann A, Muggli F, Gulich JF. Comparison of three-dimensional Navier–Stokes codes with LDA—measurements on an industrial radial pump impeller. In *Pump Machinery*, ASME FED-vol. 154, ASME: New York, 1993; 231–236.

 

16. Peng G, Guo Q, Luo X, Lin R. Calculation of three-dimensional boundary layer on hydraulic runner and the runner efficiency performance prediction. *Journal of Hydraulic Engineering* 1996; **10**:80–87.
17. Lakshminarayana B, Govindan TR. Analysis of turbulent boundary layer on cascade and rotor blades of turbomachinery. *AIAA Journal* 1981; **19**:1333–1341.
18. Wright T. *Fluid Machinery*: *Performance*, *Analysis and Design*. CRC Press: Florida, 1999; 176–192.
19. Lin R, Peng G. An advanced numerical simulation method for the rotational flow in hydraulic turbomachinery. In *Fluid Machinery*, ASME FED-vol. 222, Roratgi US, Ogut A, Hayami H (eds), ASME: New York, 1995; 173–176.
20. Denton JD. Loss mechanism in turbomachinery. *ASME Transactions Journal of Turbomachinery* 1993; **115**:11–21.
21. Lin R. *Flow Dynamics Theory of Hydraulic Machinery*. Mechanical Industry Press: Beijing, 1996; 85–96 (in Chinese).
22. Schlichting H, Gersten K. *Boundary-Layer Theory* (8th edn). Springer: Berlin, 2000; 275–296.
23. Rao SS. *Engineering Optimization*: *Theory and Practice* (3rd edn). Wiley: New York, 1996; 135–146.
24. Lee YT, Luo L. Direct method for optimization of a centrifugal compressor vaneless diffuser. *ASME Transactions Journal of Turbomachinery* 2001; **123**:73–79.
25. Lootsma FA. *Numerical Methods for Nonlinear Optimization*. Academic Press: New York, 1972; 69–97.

 